

# DEVELOPMENT OF GENERALIZED PERTURBATION THEORY CAPABILITY WITHIN THE SCALE CODE PACKAGE

**Matthew A. Jessee, Mark L. Williams, Mark D. Dehart**

Oak Ridge National Laboratory, Oak Ridge, TN 37831-6170, USA

jesseema@ornl.gov, williamsml@ornl.gov, dehartmd@ornl.gov

## ABSTRACT

Computational capability has been developed to calculate sensitivity coefficients of generalized responses with respect to cross-section data in the SCALE code system. The focus of this paper is the implementation of generalized perturbation theory (GPT) for one-dimensional and two-dimensional deterministic neutron transport calculations. GPT is briefly summarized for computing sensitivity coefficients for reaction rate ratio responses within the existing framework of the TSUNAMI sensitivity and uncertainty (S/U) analysis code package in SCALE. GPT provides the capability to analyze generalized responses related to reactor analysis, such as homogenized cross-sections, relative powers, and conversion ratios, as well as measured experimental parameters such as  $^{28}\rho$  (epithermal/thermal  $^{238}\text{U}$  capture rates) in thermal benchmarks and fission ratios such as  $^{239}\text{Pu}(n,f)/^{235}\text{U}(n,f)$  in fast benchmarks. The S/U analysis of these experimental integral responses can be used to augment the existing TSUNAMI S/U analysis capabilities for system similarity assessment and data adjustment. S/U analysis is provided for boiling water reactor pin cell as part of the Organization for Economic Cooperation and Development Uncertainty Analysis in Modeling benchmark.

*Key Words:* SCALE, GPT, sensitivity, uncertainty, lattice physics

## 1. INTRODUCTION

The SCALE code system [1] includes a sensitivity and uncertainty (S/U) analysis code package called TSUNAMI. TSUNAMI originally focused on  $k_{eff}$  responses for criticality safety analysis and included the capability to compute sensitivity coefficients using forward and adjoint solutions from three-dimensional Monte Carlo or one-dimensional (1D) discrete ordinates eigenvalue calculations. TSUNAMI also computes the implicit sensitivity effect, inherent in resonance self-shielding calculations, through the use of automatic differentiation. With the release of version 6 of SCALE, the TSUNAMI capability has been extended to include S/U analysis for eigenvalue-difference responses, or reactivity responses, coupled neutron-gamma responses for shielding applications, as well as a cross-section data adjustment tool for criticality safety validation. In this paper we discuss a further extension of the TSUNAMI code package to incorporate generalized perturbation theory (GPT) for 1D and two-dimensional (2D) deterministic transport calculations. The SCALE 1D and 2D transport codes—XSDRNPM and NEWT, respectively—have been modified to solve the generalized adjoint equation, an inhomogeneous form of the transport equation containing the singular Boltzmann operator for a critical system. Generalized adjoint solutions from the SCALE transport codes are used to compute sensitivity coefficients based on GPT expressions, which consist of *direct* effects (from data appearing directly in response functions) and *indirect* effects (from data impacting the

response through flux perturbations). Both direct and indirect effects may include *explicit* and *implicit* components. The *explicit* components describe response changes due to perturbations in multigroup cross-section data appearing in the transport equation, while the *implicit* components account for response changes caused by perturbations in cross-section self-shielding.

In the following section, the sensitivity coefficient calculations for both  $k_{eff}$  and generalized responses are summarized. S/U analysis of a boiling water reactor (BWR) pin cell is provided in Section 3 as part of the Organization for Economic Cooperation and Development (OECD) Uncertainty Analysis in Modeling (UAM) benchmark [2], followed by the conclusions in Section 4.

## 2. THEORY

### 2.1. Explicit Sensitivity Coefficients

GPT was probably initially studied by Russian scientists in the late 1950s. The first publications on the subject were by Usachev and Kadomtzev [3–4], while other seminal works are credited to Gandini, Lewins, Stacey, and Pomraning [5–8]. The expressions shown in the current paper follow the notation by Williams [9].

The forward transport equation can be written in operator form as

$$L\phi = \lambda P\phi, \quad (1)$$

where  $\phi$  represents the neutron flux,  $L$  all of the transport operator except the fission term,  $\lambda$  the eigenvalue of the transport equation, and  $P$  the fission term of the transport operator. In this form, the forward transport equation is written as an eigenvalue problem in which the neutron flux is an eigenvector associated with the eigenvalue  $\lambda$ . The largest eigenvalue (equal to  $1/k_{eff}$ ) and its associated eigenvector is referred to as the forward fundamental mode solution.

The adjoint transport equation can be derived by defining an inner product for the forward transport equation as the integration over all phase space (i.e., volume, energy, and direction). The adjoint equation can be written in operator form as

$$L^\dagger \phi^\dagger = \lambda P^\dagger \phi^\dagger, \quad (2)$$

where  $\phi^\dagger$  represents the adjoint flux, and  $L^\dagger$  and  $P^\dagger$  are the adjoint operators to  $L$  and  $P$ . The eigenvalues for the adjoint equation are equal to the eigenvalues for the forward equation. The adjoint eigenvector associated with the largest eigenvalue is referred to as the adjoint fundamental mode solution.

TSUNAMI uses the solutions to the forward and adjoint transport equations to calculate *explicit* eigenvalue sensitivity coefficients to multigroup cross-section data. The explicit sensitivity coefficients characterize the first-order accurate change in eigenvalue due to changes in the

multigroup cross-sections. The explicit eigenvalue sensitivity coefficient to a given multigroup cross-section  $\alpha$ ,  $S_{\lambda, \alpha}$ , is given as

$$S_{\lambda, \alpha} \equiv \frac{1}{\lambda} \frac{\partial \lambda}{\partial \alpha} \alpha = \frac{1}{\lambda} \frac{\langle \phi^\dagger, (\frac{\partial L}{\partial \alpha} \alpha - \lambda \frac{\partial P}{\partial \alpha} \alpha) \phi \rangle}{\langle \phi^\dagger, P \phi \rangle} \quad (3)$$

or in terms of  $k_{eff}$  sensitivities as

$$S_{k_{eff}, \alpha} \equiv S_{\lambda, \alpha} \left( \frac{1}{\lambda} \frac{\partial \lambda}{\partial k_{eff}} k_{eff} \right) = -S_{\lambda, \alpha}. \quad (4)$$

The *explicit* sensitivity coefficient captures both the *direct* change in the eigenvalue due to the perturbations of the  $L$  and  $P$  operators and the *indirect* change due to neutron flux perturbations.

Explicit sensitivity coefficients to system responses other than  $k_{eff}$  have expressions similar to Eq. (3) and have been derived in [9] using both standard adjoint and variation approaches. Defining a system response as a ratio of inner products of the forward neutron flux, that is,

$$R = \frac{\langle H_1, \phi \rangle}{\langle H_2, \phi \rangle}, \quad (5)$$

the explicit response sensitivity coefficient is given as

$$S_{R, \alpha} \equiv \frac{1}{R} \frac{\partial R}{\partial \alpha} \alpha = \frac{1}{\langle H_1, \phi \rangle} \langle \frac{\partial H_1}{\partial \alpha} \alpha, \phi \rangle - \frac{1}{\langle H_2, \phi \rangle} \langle \frac{\partial H_2}{\partial \alpha} \alpha, \phi \rangle - \langle \Gamma^\dagger, (\frac{\partial L}{\partial \alpha} \alpha - \lambda \frac{\partial P}{\partial \alpha} \alpha) \phi \rangle. \quad (6)$$

In this equation, the first two terms on the right-hand side represent the *direct* change in the system response due to the cross-section perturbation in the response function, and the final term represents the *indirect* change due to the perturbation of the neutron flux. In the indirect effect term, the adjoint fundamental mode has been replaced with the so-called generalized adjoint  $\Gamma^\dagger$ , which is the solution to the following adjoint equation:

$$L^\dagger \Gamma^\dagger = \lambda P^\dagger \Gamma^\dagger + S^\dagger. \quad (7)$$

The generalized adjoint equation contains a generalized source term on the right-hand side that is not present in the adjoint fundamental mode equation (Eq. [2]). The generalized adjoint source is computed as the functional derivative of the system response  $R$  with respect to the forward neutron flux, that is,

$$S^\dagger \equiv \frac{1}{R} \frac{\partial R}{\partial \phi} = \frac{H_1}{\langle H_1, \phi \rangle} - \frac{H_2}{\langle H_2, \phi \rangle}. \quad (8)$$

In this expression, the functional derivative contains a  $1/R$  normalization so that relative sensitivity coefficients can be easily computed (i.e., a relative change in the response due to a relative change in the cross-sections).

Because of the presence of the fundamental mode eigenvalue in Eq. (7), the generalized adjoint equation represents a singular system of equations that contains an infinite number of solutions. The generalized adjoint can be expressed as a linear combination of the adjoint fundamental mode solution and a particular inhomogeneous adjoint solution with no fundamental mode. Therefore, the generalized adjoint can be written as

$$\Gamma^\dagger = \Gamma_p^\dagger + \gamma \phi^\dagger, \quad (9)$$

where  $\gamma$  is a scalar variable that represents an arbitrary amount of the adjoint fundamental mode solution. To determine a unique solution to Eq. (9),  $\gamma$  is usually chosen such that the generalized adjoint solution is orthogonal to the forward neutron fission source, that is,

$$\langle \Gamma_p^\dagger + \gamma \phi^\dagger, P\phi \rangle = 0 \Rightarrow \gamma = -\frac{\langle \Gamma_p^\dagger, P\phi \rangle}{\langle \phi^\dagger, P\phi \rangle}. \quad (10)$$

This orthogonality condition can be derived by imposing the constraint that the response is stationary (i.e., insensitive) to perturbations in the eigenvalue when determining the first-order accurate changes in the system response. In both XSDRNPM and NEWT, the value of  $\gamma$  is determined by standard fundamental mode removal techniques discussed in [9].

## 2.2. Implicit Sensitivity Coefficients

The explicit sensitivity coefficients described in the previous section characterize the first-order change in a system response due to changes in multigroup cross-sections used in the transport model. The multigroup cross-sections used in the transport model are typically prepared by unit cell calculations that simulate important spatial and energy resonance self-shielding effects. Because cross-section uncertainty data are typically provided for unshielded cross-sections, the sensitivity coefficients need to be modified to account for the implicit self-shielding effects in the unit cell calculations [10].

In SCALE, sensitivity versions of the resonance processing codes are used to compute sensitivity coefficients of the shielded cross-sections with respect to input data used in the unit cell calculations. The changes in the input data can be related back to changes in the unshielded multigroup cross-section data through the use of the chain rule. The final sensitivity coefficient, referred to as the complete sensitivity coefficient, is given as

$$S_{R,\alpha} = S_{R,\alpha}^{\text{explicit}} + S_{R,\alpha}^{\text{implicit}} = \frac{1}{R} \frac{\partial R}{\partial \alpha} \alpha + \sum_{\alpha'} \frac{1}{R} \frac{\partial R}{\partial \alpha'} \alpha' \sum_{\omega} \left( \frac{1}{\alpha'} \frac{\partial \alpha'}{\partial \omega} \omega \right) \left( \frac{1}{\omega} \frac{\partial \omega}{\partial \alpha} \alpha \right). \quad (12)$$

The first term on the right-hand side of Eq. (12) represents the explicit sensitivity coefficient, while the second term represents the implicit sensitivity coefficient. In the implicit term, the first

summation is over all multigroup cross-sections,  $\alpha'$ , while the second summation is over all input parameters,  $\omega$ . The final sensitivity coefficient on the right-hand side relates the changes in the input parameters back to the unshielded multigroup cross-sections. It is important to note that both the explicit and implicit sensitivity coefficient terms contain direct effect components from the cross-section perturbation and indirect effect components from the perturbation in the neutron flux. The complete sensitivity coefficients are used with cross-section covariance data to calculate the response variance as

$$\frac{VAR(R)}{R^2} = \sum_{\alpha} S_{R,\alpha} \sum_{\alpha'} \frac{COV(\alpha, \alpha')}{(\alpha)(\alpha')} S_{R,\alpha'}, \quad (13)$$

where  $VAR(R)$  represents the absolute variance in response  $R$  and  $COV(\alpha, \alpha')$  represents the absolute covariance between cross-section  $\alpha$  and  $\alpha'$ .

### 3. BWR PIN CELL ANALYSIS

The TSUNAMI GPT capability has been applied to the BWR fuel pin model from Phase 1-1 of the OECD UAM benchmark. The BWR fuel pin model consists of a single  $UO_2$  fuel pin (2.93% enriched  $^{235}U$ ) modeled at hot zero power (HZP) with reflective boundary conditions. The HZP moderator and fuel temperature is 552.833 K, and the moderator density is 753.978 kg/m<sup>3</sup>.

BWR fuel pin sensitivity calculations were performed using both the XSDRNPM and NEWT transport models. For the XSDRNPM model, the moderator region was modeled as a cylinder with white boundary conditions. In both cases, 238-group self-shielded cross-sections were prepared using BONAMIST and CENTRM for the unit cell calculation with ENDF/B-VI cross-sections. New for the version 6 release of SCALE, BONAMIST uses full-range Bondarenko factors to compute sensitivity coefficients for all energy groups used in the implicit sensitivity coefficient calculation. In this approach, BONAMIST calculates full-range sensitivity data along with the self-shielded cross-section data in the unresolved resonance range. The self-shielded cross-section data below the unresolved resonance range are calculated using CENTRM. For the NEWT calculations, spatial-angle mesh refinement studies were completed to determine the appropriate mesh for the sensitivity analysis. The NEWT calculations were completed using an  $S_{16}$  angular quadrature and the spatial mesh shown in Figure 1. The XSDRNPM calculations were completed using an  $S_{16}$  angular quadrature and 4 spatial mesh intervals per material region.

As part of the OECD UAM benchmark specification, S/U analysis is requested for  $k_{eff}$  as well as one-group fission and absorption cross-sections for  $^{235}U$  and  $^{238}U$ . These values are provided in Table I for both XSDRNPM calculations in TSUNAMI-1D and NEWT calculations in TSUNAMI-2D. The response uncertainty values were computed using the 44GROUPCOV cross-section covariance library from SCALE 6. Both the computed response values and response uncertainty values are in good agreement between the two transport models. The one-group effective microscopic cross-sections were calculated using the 238-group flux spectra *in the fuel region*. For one-group homogenized cross-sections, the cell-weighted flux spectra should be used.

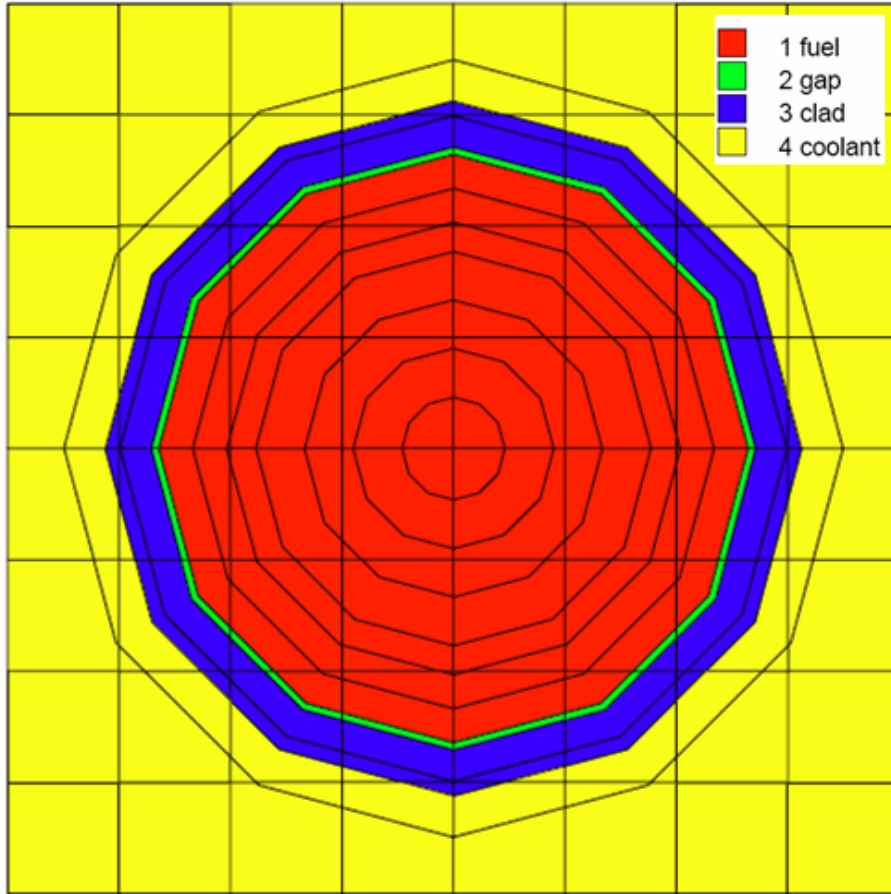
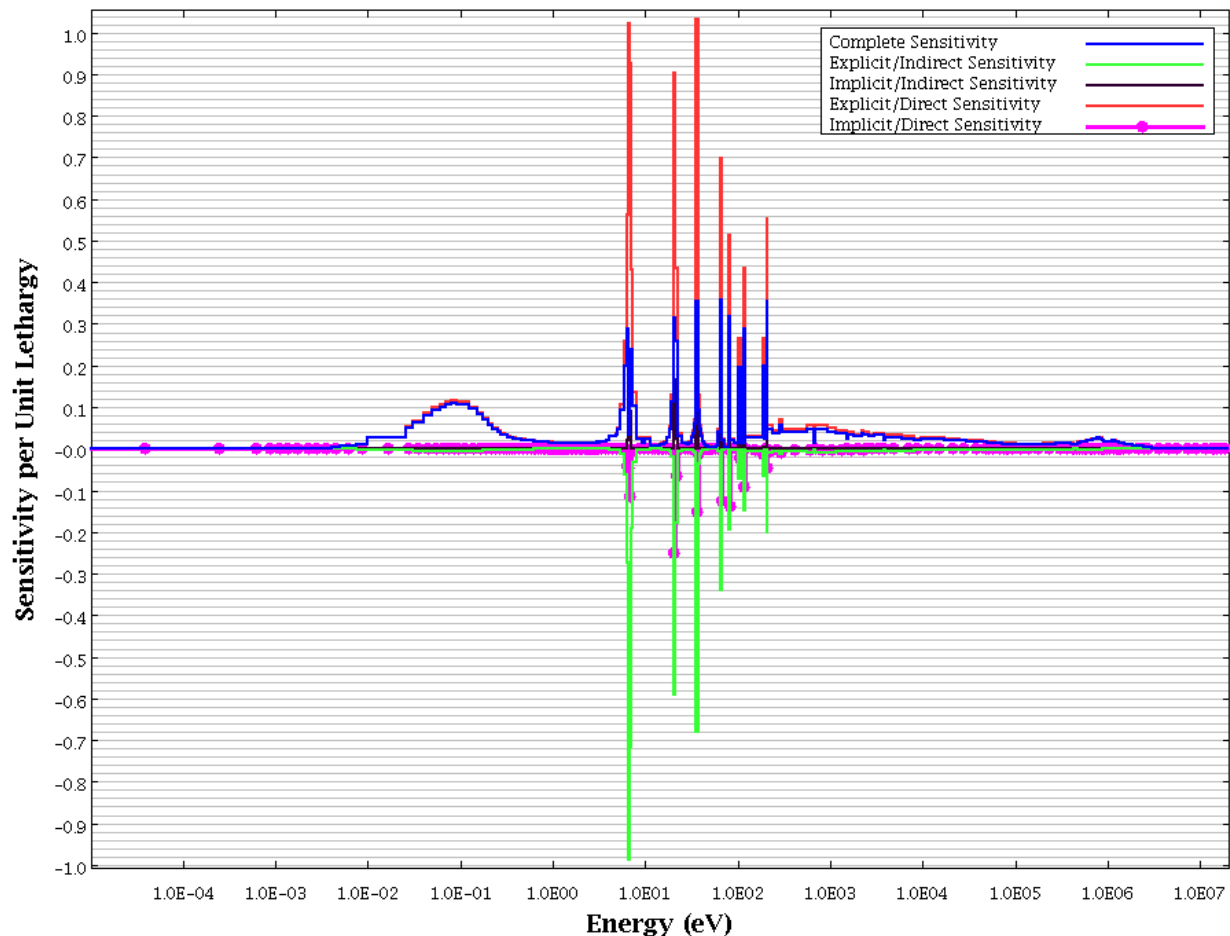


Figure 1. NEWT spatial mesh for BWR pin cell model.

Table I. Response values for BWR pin cell at HZP.

Response	TSUNAMI-1D using XSDRNPM		TSUNAMI-2D using NEWT	
	Value	1 $\sigma$ (%)	Value	1 $\sigma$ (%)
$k_{eff}$	1.33612	0.522	1.33952	0.521
$^{235}\text{U}$ (n, $\gamma$ )	10.6421 b	1.67	10.6186 b	1.66
$^{235}\text{U}$ (n,f)	49.0398 b	1.05	49.0353 b	1.04
$^{235}\text{U}$ [(n, $\gamma$ )+(n,f)]	59.6819 b	2.21	59.6538 b	2.31
$^{238}\text{U}$ (n, $\gamma$ )	0.83995 b	1.32	0.83014 b	1.34
$^{238}\text{U}$ (n,f)	0.09485 b	3.97	0.09490 b	4.02
$^{238}\text{U}$ [(n, $\gamma$ )+(n,f)]	0.93481 b	3.74	0.92503 b	3.79

To illustrate the different sensitivity coefficient components computed in TSUNAMI, the sensitivity coefficients of the collapsed one-group  $^{238}\text{U}$  ( $n,\gamma$ ) with respect to the  $^{238}\text{U}$  ( $n,\gamma$ ) multigroup data are plotted as a function of energy in Figure 2. The complete sensitivity coefficient is plotted in blue along with the four major sensitivity components: the explicit-indirect component is plotted in green, the implicit-indirect component is plotted in black, the explicit-direct component is plotted in red, and the implicit-direct component is plotted in pink. The  $^{238}\text{U}$  ( $n,\gamma$ ) cross-section provides the only data with a direct effect for this response. The explicit-direct component considers only the perturbation of the multigroup data appearing in the response function. Therefore, the explicit-direct sensitivity coefficient is always positive because the one-group flux-weighted cross-section varies directly with changes in the multigroup data (i.e., an increase in the multigroup cross-section data will increase the flux-weighted average cross-section). Because the explicit-direct component does not account for changes in the neutron flux, the magnitude of the explicit-direct sensitivity coefficient is largest at the peaks of the low-lying resonances of  $^{238}\text{U}$ .



**Figure 2. One-group  $^{238}\text{U}$  ( $n,\gamma$ ) sensitivity coefficient components with respect to the multigroup  $^{238}\text{U}$  ( $n,\gamma$ ) data.**

Accounting for the change in the multigroup neutron flux, the explicit-indirect sensitivity coefficients are in the opposite direction of the explicit-direct component. Increasing the multigroup cross-section enhances the local depression of the neutron flux in the  $^{238}\text{U}$  resonance groups. This decrease in the neutron flux in turn decreases the value of the response. As with the explicit-direct component, the magnitude of the explicit-indirect component is the largest near the low-lying resonances of  $^{238}\text{U}$ .

Barely visible on the plot in Figure 2 are the implicit-indirect and implicit-direct sensitivity components. The implicit sensitivities are large near the cross-section resonances due to increased self-shielding effects. The complete sensitivity coefficient plot is the summation of each of the four sensitivity components. It should be noted that the complete sensitivity coefficient is considerably smaller than the explicit-direct sensitivity coefficient. Accounting for the flux perturbation through the GPT calculation provides a more accurate estimate of the sensitivity coefficients, which impacts the uncertainty analysis and validation of the critical system.

Complete sensitivity coefficients by nuclide are provided in Table II for each response. The large, negative sensitivity coefficients for  $^{238}\text{U}$  are due to the dominant role of resonance absorption in the fuel pin. The large  $^1\text{H}$  sensitivities indicate a strong indirect dependence of the fuel energy spectra due to the hydrogen cross-section as well as a strong implicit dependence due to the self-shielding effect in the unit cell calculation. The sensitivity coefficients provided in Table II were verified using a series of direct perturbation calculations with each nuclide number density perturbed by  $\pm 5\%$ . The sensitivity coefficients to  $^{234}\text{U}$  and other cladding materials were less than  $10^{-3}$  and omitted from Table II.

**Table II. Nuclide sensitivity coefficients for each response.**

Nuclide	Sensitivity coefficients for indicated response				
	$k_{eff}$	$^{235}\text{U} (n,\gamma)$	$^{235}\text{U} (n,f)$	$^{238}\text{U} (n,\gamma)$	$^{238}\text{U} (n,f)$
$^{238}\text{U}$	-2.09E-01	-1.23E-01	-1.43E-01	-1.95E-01	-1.12E-01
$^{235}\text{U}$	1.58E-01	-5.40E-01	-6.81E-01	-1.48E-01	1.39E-01
$^1\text{H}$	1.19E-01	5.94E-01	7.70E-01	1.66E-01	1.03E-01
$^{16}\text{O}$ (fuel region)	-1.35E-02	2.05E-02	2.06E-02	3.92E-02	-3.41E-02
Zr	-1.35E-02	6.42E-03	5.25E-03	9.52E-03	-4.89E-02
$^{16}\text{O}$ (moderator)	-2.78E-03	2.00E-02	2.15E-02	1.70E-02	-2.54E-02

In addition to the sensitivity coefficients shown in Table II, TSUNAMI computes the contributions to the response uncertainty due to the cross-section covariance data. Table III lists the top 15 cross-section covariance matrices that contribute to  $k_{eff}$  uncertainty. Likewise, Table IV lists the top 15 cross-section covariance matrices that contribute to the one-group  $^{235}\text{U} (n,f)$  uncertainty. In both cases, the top 15 contributors represent more than 99% of the total uncertainty in the response due to the cross-section covariance data. The total uncertainty is computed by taking the square root of the sum of the squares of each uncertainty contribution.

**Table III. Uncertainty contribution in  $k_{eff}$ .**

<b>Nuclide-Reaction</b>	<b>Nuclide-Reaction</b>	<b>Percent delta-k/k due to this matrix</b>
$^{238}\text{U} (n,\gamma)$	$^{238}\text{U} (n,\gamma)$	3.29E-01
$^{235}\text{U} \bar{\nu}$	$^{235}\text{U} \bar{\nu}$	2.71E-01
$^{235}\text{U} (n,\gamma)$	$^{235}\text{U} (n,\gamma)$	1.81E-01
$^{238}\text{U} (n,n')$	$^{238}\text{U} (n,n')$	1.27E-01
$^{235}\text{U} (n,f)$	$^{235}\text{U} (n,\gamma)$	1.13E-01
$^{235}\text{U} (n,f)$	$^{235}\text{U} (n,f)$	9.39E-02
$^{235}\text{U} \text{ chi}$	$^{235}\text{U} \text{ chi}$	8.54E-02
$^{238}\text{U} \bar{\nu}$	$^{238}\text{U} \bar{\nu}$	7.91E-02
Zr (n, $\gamma$ )	Zr (n, $\gamma$ )	5.53E-02
$^1\text{H} (n,\gamma)$	$^1\text{H} (n,\gamma)$	2.89E-02
$^1\text{H} (n,n)$	$^1\text{H} (n,n)$	2.54E-02
$^{238}\text{U} (n,n)$	$^{238}\text{U} (n,\gamma)$	-2.11E-02
$^{238}\text{U} (n,n)$	$^{238}\text{U} (n,n)$	1.96E-02
$^{238}\text{U} (n,f)$	$^{238}\text{U} (n,f)$	1.77E-02
$^{238}\text{U} (n,n)$	$^{238}\text{U} (n,n')$	-1.61E-02
	<b>Total</b>	<b>5.21E-01</b>

**Table IV. Uncertainty Contribution in one-group  $^{235}\text{U} (n,f)$ .**

<b>Nuclide-Reaction</b>	<b>Nuclide-Reaction</b>	<b>Percent delta-R/R due to this matrix</b>
$^{238}\text{U} (n,n')$	$^{238}\text{U} (n,n')$	7.82E-01
$^{235}\text{U} \text{ chi}$	$^{235}\text{U} \text{ chi}$	4.17E-01
$^1\text{H} (n,n)$	$^1\text{H} (n,n)$	3.95E-01
$^{238}\text{U} (n,\gamma)$	$^{238}\text{U} (n,\gamma)$	2.66E-01
$^{235}\text{U} (n,\gamma)$	$^{235}\text{U} (n,\gamma)$	1.53E-01
$^{235}\text{U} (n,f)$	$^{235}\text{U} (n,f)$	1.37E-01
$^{235}\text{U} (n,f)$	$^{235}\text{U} (n,\gamma)$	1.29E-01
$^{238}\text{U} (n,n)$	$^{238}\text{U} (n,n')$	-8.41E-02

**Table IV. Uncertainty Contribution in one-group  $^{235}\text{U}$  (n,f) (continued).**

Nuclide-Reaction	Nuclide-Reaction	Percent delta-R/R due to this matrix
Zr (n,n')	Zr (n,n')	8.23E-02
$^{16}\text{O}$ (n,n)	$^{16}\text{O}$ (n,n)	6.94E-02
Zr (n, $\gamma$ )	Zr (n, $\gamma$ )	3.80E-02
$^{238}\text{U}$ chi	$^{238}\text{U}$ chi	3.76E-02
$^1\text{H}$ (n, $\gamma$ )	$^1\text{H}$ (n, $\gamma$ )	2.61E-02
$^{238}\text{U}$ (n,n)	$^{238}\text{U}$ (n, $\gamma$ )	-1.86E-02
$^{238}\text{U}$ (n,2n)	$^{238}\text{U}$ (n,2n)	1.50E-02
	<b>Total</b>	<b>1.04E+00</b>

As seen in Table III, negative uncertainty contributions exist due to anti-correlations in the cross-section covariance data. The negative uncertainty contributions are subtracted when computing the total response uncertainty. The top contributor to  $k_{eff}$  uncertainty is the  $^{238}\text{U}$  (n, $\gamma$ ) cross-section. This is due to large  $k_{eff}$  sensitivities to the  $^{238}\text{U}$  (n, $\gamma$ ) cross-section in the epithermal energy range where the relative standard deviation of the multigroup cross-sections range from 2% to 4%. Although  $k_{eff}$  sensitivities to  $^1\text{H}$  cross-sections are comparable in magnitude to  $^{238}\text{U}$  cross-section sensitivities, the  $^1\text{H}$  cross-section uncertainty contributions are much smaller. This is because the  $^1\text{H}$  cross-sections have smaller uncertainty. The one-group  $^{235}\text{U}$  (n,f) response sensitivity to  $^{238}\text{U}$  (n, $\gamma$ ) is smaller than for  $k_{eff}$ , primarily because the  $^{238}\text{U}$  (n, $\gamma$ ) cross-section can only indirectly change the one-group  $^{235}\text{U}$  (n,f) response due to perturbations in the fuel flux spectra. Consequently, the uncertainty contribution from the  $^{238}\text{U}$  (n, $\gamma$ ) cross-section is smaller for the  $^{235}\text{U}$  (n,f) response than for  $k_{eff}$ . Similarly, the uncertainty contribution from the  $^{235}\text{U}$  (n,f) cross-section is larger for the one-group  $^{235}\text{U}$  (n,f) response than for  $k_{eff}$  due its larger direct-effect sensitivity.

### 3. CONCLUSIONS

Computational capability has been developed in SCALE to calculate sensitivity coefficients for ratio responses in a critical system. The new capability employs generalized perturbation theory to determine the indirect effect of the flux perturbation due to multigroup cross-section perturbations for 1D and 2D deterministic transport calculations. The generalized adjoint solution can be used to calculate indirect effect sensitivity coefficients within the existing framework of TSUNAMI in SCALE.

In this paper, the TSUNAMI GPT capability was applied to selected responses of the BWR pin of the OECD UAM benchmark. ENDF/B-VI cross-section data were used for the calculations, along with the 44GROUPCOV multigroup cross-section covariance library in SCALE 6. For the BWR pin model, response sensitivities and uncertainties were quantified for system  $k_{eff}$  and one-group effective cross-sections for  $^{235}\text{U}$  and  $^{238}\text{U}$ . The TSUNAMI GPT capability provides a

useful means of quantifying homogenized few-group cross-section uncertainties to facilitate reactor-core simulation uncertainty analysis.

## ACKNOWLEDGMENTS

This work was supported by Oak Ridge National Laboratory through Laboratory Directed Research Development project number 507-003.

## REFERENCES

1. *SCALE: A Modular Code System for Performing Standardized Computer Analyses for Licensing Evaluations*, ORNL/TM-2005/39, Version 6, Vols. I–III, February 2009. Available from Radiation Safety Information Computational Center at Oak Ridge National Laboratory as CCC-725.
2. K. Ivanov, M. Avramova, I. Kodeli, and E. Satori, “Benchmark for Uncertainty Analysis in Modeling (UAM) for Design, Operation, and Safety Analysis of LWRs,” NEA/NSC/DOC(2007)23.
3. L. N. Usachev, “Perturbation theory for the breeding ratio and for other number ratios pertaining to various reactor processes,” *J. Nucl. Energy, Parts A/B* **18**, p. 571, 1964.
4. B. B. Kadomtzev, “On the importance function in radiative energy transport,” *Dokl. An. SSSR* **113**(3), 1957.
5. A. Gandini, “A generalized perturbation method for bilinear functionals of the real and adjoint neutron fluxes,” *J. Nucl. Energy* **21**, p. 755, 1967.
6. J. Lewins, *Importance: The Adjoint Function*, Pergamon Press, Oxford, 1965.
7. W. Stacey, *Variational Methods in Nuclear Reactor Physics*, Academic Press, New York, 1974.
8. G. Pomraning, “Variational principle for eigenvalue equations,” *J. Math. Phys.* **8**, p. 149, 1967.
9. M. L. Williams, “Perturbation Theory for Reactor Analysis,” *CRC Handbook of Nuclear Reactor Calculations*, pp. 63–188, CRC Press, 1986.
10. M. L. Williams and B. T. Rearden, “SCALE-6 Sensitivity/Uncertainty Methods and Covariance Data,” *Nuclear Data Sheets* **109**(12), p. 2796, 2009.